# Binding and Cytotoxicity of HPMA Copolymer Conjugates to Lymphocytes Mediated by Receptor-Binding Epitopes

**Aijun Tang,[1] Pavla Kopečková,[1,2] and Jindřich Kopeček[1,2,3]**

*Received September 17, 2002; accepted December 4, 2002*

***Purpose.*** Studies on the recognition of epitopes presented on a template peptide showed the potential of nonapeptide-related sequences to act as biorecognition sites for the B-cell CD21 receptor. This study was intended to evaluate the capability of three epitope sequences to mediate specific cell binding and to enhance the cytotoxicity of HPMA copolymer conjugates.

***Methods.*** HPMA copolymer conjugates were synthesized containing three different epitopes at various contents and either a fluorescent marker or doxorubicin (DOX). The binding and cytotoxicity of the conjugates to $CD21^+$ Raji B cells and $CD21^-$ HSB-2 T cells were evaluated.

***Results.*** The epitope-containing conjugates were found to bind to Raji cells at different apparent affinities depending on epitope structure and content. The conjugates generally possessed higher affinities for Raji cells than for HSB-2 cells. Targeted HPMA copolymer–DOX conjugates exhibited higher cytotoxicities than the nontargeted conjugate, likely indicative of enhanced internalization by receptor-mediated endocytosis. HSB-2 cells were more sensitive to both free and polymer-bound DOX than Raji cells; however, the enhancement of cytotoxicity of the conjugates by incorporation of epitopes was more pronounced for Raji cells.

***Conclusions.*** The results verified the concept of using receptor-binding epitopes as targeting moieties in HPMA copolymer conjugates for the delivery of anticancer drugs to lymphoma cells.

**KEY WORDS:** HPMA copolymer conjugates; epitope; CD21 receptor; binding affinity; cytotoxicity; lymphocytes.

## INTRODUCTION

Leukemia, lymphoma, and myeloma are related cancers characterized by the uncontrolled growth of cells with similar functions and origins. These blood-related cancers accounted for about 8.6% of 1,268,000 new cancer cases diagnosed in the United States in 2001 and were responsible for nearly 11% of the total deaths from cancers (1). "Lymphoma" is a broad term encompassing a group of cancers that originate in the lymphatic system. Current treatments for these blood-related cancers include chemotherapy, radiation therapy, a combination of chemo- and radiotherapy, immunotherapy, or, in specific cases, high-dose chemotherapy followed by bone marrow or stem cell transplantation. Chemotherapy is largely responsible for the dramatic improvement in the treatment of these cancers. However, it is often accompanied by unwanted side effects. The development of new chemotherapy drugs has greatly increased the cure rates and remission period and has reduced the side effects of some malignancies; however, improvement of the therapeutic index of existing anticancer drugs is highly desirable. One promising approach to improving chemotherapy is to use drug delivery systems.

The water-soluble polymer system N-(2-hydroxypropyl)methacrylamide (HPMA) copolymers has been studied for nearly two decades as a carrier for low-molecular-weight drugs to improve cancer chemotherapy (2,3). Covalent binding of anticancer drugs to HPMA copolymers can simultaneously improve the solubility of the drugs and prolong their blood circulation time. More importantly, polymer-bound drugs are believed to have increased accumulation in solid tumors as a result of enhanced permeability and a retention (EPR) effect (4). In addition, HPMA copolymer-bound doxorubicin (DOX) has been shown to overcome P-glycoprotein-associated multidrug resistance (5) and to have greater efficacy than the free drug (6,7). Incorporation of targeting moieties in the conjugate system often results in an improvement in the therapeutic efficacy of polymer-bound drugs by facilitating binding of the conjugates to target cells and promoting conjugate internalization. A concomitant benefit with the use of targeting moieties is a lowered nonspecific toxicity of the drug. Examples of targeting moieties that have been used in HPMA copolymer conjugate system include carbohydrates (8) and antibodies and antibody fragments (9,10). In addition to the well-established targeting strategies, a rather new approach is to use receptor-binding epitopes as the biorecognition sites in HPMA copolymer conjugates that mediate specific interactions of the conjugates with receptor-bearing cells. Advantageous properties of small epitopes for targeting moieties include the possibility of multivalent interactions if multiple epitope molecules are linked to each macromolecular chain, and probably easier transcompartmental transport of the epitope-containing conjugates because of their small size relative to the large antibody-containing conjugates.

The CD21 receptor is a 145-kDa integral membrane glycoprotein found mainly on mature B cells (11) and on certain T cells (12). The CD21 or CD21-like receptor was shown to overexpress on a subset of cancerous cells relative to normal cells (13,14). This observation indicated that CD21 might be a useful target for the delivery of anticancer drugs to $CD21^+$ malignant cells. Epstein–Barr virus (EBV) was found to bind to the CD21/EBV receptor on B cells through its main envelope glycoprotein gp350/220 (15). Specifically, a nonapeptide (NP) sequence (EDPGFFNVE) close to the N-terminus of gp350/220 seemed to play an important role (16). Previous work using NP-containing HPMA copolymer conjugates showed that the NP sequence induced specific binding of the conjugates to B and T cells and that the binding affinities seemed to increase with increasing peptide content in the conjugates (17). Further studies investigated the recognition of NP-related epitopes presented on coiled coil stem loop peptides by purified soluble CD21 receptor and $CD21^+$ Raji cells (18). The results indicated that two other epitope sequences, peptides "D" (EDPGFFNVEIPEF) and "F" (EFGLDPGNFVEGF), might also act as biorecognition sites

[1] Department of Pharmaceutics and Pharmaceutical Chemistry, University of Utah, Salt Lake City, Utah 84112.

[2] Department of Bioengineering, University of Utah, Salt Lake City, Utah 84112.

[3] To whom correspondence should be addressed. (e-mail: Jindrich.Kopecek@m.cc.utah.edu)

0724-8741/03/0300-0360/0 © 2003 Plenum Publishing Corporation

in the HPMA copolymer conjugate system for targeted delivery of anticancer drugs.

In this work, two sets of epitope (EP)-containing HPMA copolymer conjugates were synthesized, HPMA copolymer–fluorescein isothiocyanate–EP (P–FITC–EP) and HPMA copolymer–doxorubicin–EP (P–DOX–EP) conjugates. In the P–FITC–EP conjugates, the epitopes were linked to the polymer backbone via two oligopeptide spacers, lysosomal enzyme cleavable "GFLG" and nondegradable "GG" spacers. In the P–DOX–EP conjugates, only the tetrapeptide spacer "GFLG" was used. Binding of the P–FITC–EP conjugates and cytotoxicity of the P–DOX–EP conjugates to $CD21^+$ Raji (B) cells and $CD21^-$ HSB-2 (T) cells were evaluated. The influence of the epitope structure and epitope content on the cell-binding affinity was investigated.

## MATERIALS AND METHODS

### Materials

Wang resin (*p*-benzyloxybenzyl alcohol resin) (100–200 mesh) was purchased from Calbiochem-Novabiochem Corp. (San Diego, CA). Diisopropylethylamine (DIPEA) and triisopropylsilane (TIS) were from Aldrich (Milwaukee, WI). Trifluoroacetic acid (TFA), 3-(4,5-dimethylthiazol-2-yl)-2,5-diphenyltetrazolium bromide (MTT), cathepsin B (bovine spleen), glutathione (GSH), N-benzoyl-Phe-Val-Arg *p*-nitroanilide hydrochloride (Bz-Phe-Val-Arg-NAp), RPMI 1640 medium, Iscove's modified Dulbecco's medium, and Dulbecco's phosphate-buffered saline (DPBS) were purchased from Sigma (St. Louis, MO). Fetal bovine serum (FBS) was obtained from Hyclone (Logan, UT). BCA protein assay kit was from Pierce (Rockford, IL). Doxorubicin (DOX) hydrochloride was a kind gift from Dr. A. Suarato at Pharmacia-Upjohn (Milano, Italy). Sephadex LH-20 was from Amersham Pharmacia Biotech (Piscataway, NJ). Other reagents and solvents used were ACS grade or higher.

The Raji B-cell line (human Burkitt's lymphoma) and CCRF-HSB-2 (HSB-2 in short) T-cell line (human acute lymphoblastic leukemia) were obtained from the American Type Culture Collection (ATCC, Rockville, MD).

### Solid-Phase Peptide Synthesis

The epitope peptides (D, NP, F) were synthesized manually using standard Fmoc chemistry on the Wang resin. The peptides were cleaved from the resin with a mixture of 95% TFA, 2.5% TIS, and 2.5% $H_2O$ (v/v). The identity of the peptides was verified by matrix-assisted laser desorption/ionization time-of-flight mass spectrometry (MALDI-TOF MS), RP-HPLC, and amino acid analysis.

### Synthesis of Polymer Precursors

N-(2-Hydroxypropyl)methacrylamide (HPMA) (19), N-methacryloylglycylglycine *p*-nitrophenyl ester (MA–GG–ONp) (20), N-methacryloylglycylphenylalanylleucyl glycine *p*-nitrophenyl ester (MA–GFLG–ONp) (21), and 5-[3-(methacryloylaminopropyl)thioureidyl] fluorescein (MA–AP–FITC) (22) were synthesized as previously described. Polymer precursors (PP) were prepared by radical copolymerization of corresponding monomers: HPMA, MA–GG–ONp, and MA–AP–FITC for P–FITC–GG–ONp (PP1); HPMA, MA–GFLG–ONp, and MA–AP–FITC for P–FITC–GFLG–ONp (PP2); HPMA and MA–GG–ONp for P–GG–ONp (PP3); and HPMA and MA–GFLG–ONp for P–GFLG–ONp (PP4). Copolymers were analyzed by size-exclusion chromatography on an ÄKTA FPLC system (Pharmacia) using a Superose 6 analytical column (16/30) (Pharmacia). The content of ONp and FITC groups was determined by UV/vis spectrophotometry (Table I).

### Synthesis of Polymer Conjugates

#### *Synthesis of Polymer Conjugates Containing FITC and EP*

PP1 and PP2 were used for the synthesis of conjugates containing FITC and epitopes bound to the polymer backbone via "GG" (C1 to C3) and "GFLG" spacers (C4 to C6), respectively (Fig. 1A) following a procedure modified from a previously described protocol (17). A typical synthesis is described as follows.

PP1 (50 mg, 20 μmol ONp) and epitope D (43 mg, 26 μmol) were dissolved in DMF (0.4 ml). DIPEA (30 μl, 177 μmol) diluted in DMF (1:1 v/v) was added slowly using a Hamilton syringe while stirring. The reaction mixture was stirred at room temperature in the dark overnight. After unreacted ONp groups were deactivated with 1-amino-2-propanol (2 μl), the mixture was diluted into DI water. The solution was dialyzed intensively and then lyophilized, yielding 72 mg (86%) of P–FITC–GG–[D]-1 with a high D content

**Table I.** Composition of Polymer Precursors

| Polymer precursor | Structure | $M_w$[a] (kDa) | PD[b] | ONp content[c] (mmol/g) | ONp content[c] (mol%) | FITC content[d] (mmol/g) | FITC content[d] (mol%) |
|---|---|---|---|---|---|---|---|
| PP1 | P–FITC–GG–ONp | 18.7 | 1.2 | 0.40 | 6.6 | 0.13 | 2.1 |
| PP2 | P–FITC–GFLG–ONp | 21.4 | 1.5 | 0.38 | 7.0 | 0.13 | 2.4 |
| PP3 | P–GG–ONp | 18.5 | 1.2 | 0.59 | 9.4 | — | — |
| PP4 | P–GFLG–ONp | 16.7 | 1.2 | 0.44 | 7.8 | — | — |

[a] $M_w$: Weight-average molecular weight determined by size-exclusion chromatography after aminolysis of ONp groups with 1-amino-2-propanol.

[b] PD: Polydispersity, the ratio of weight-average and number-average molecular weights.

[c] Extinction coefficients for ONp group: 9500 $M^{-1}$ $cm^{-1}$ ($\lambda_{max}$ ~273 nm in DMSO–1%$CH_3COOH$) in the absence of FITC, and 18,000 $M^{-1}$ $cm^{-1}$ ($\lambda_{max}$ ~ 400 nm in borate buffer, pH 9.2) in precursors containing both FITC and ONp groups.

[d] Extinction coefficient for FITC group: 82,000 $M^{-1}$ $cm^{-1}$ ($\lambda_{max}$ ~494 nm in borate buffer, pH 9.2).

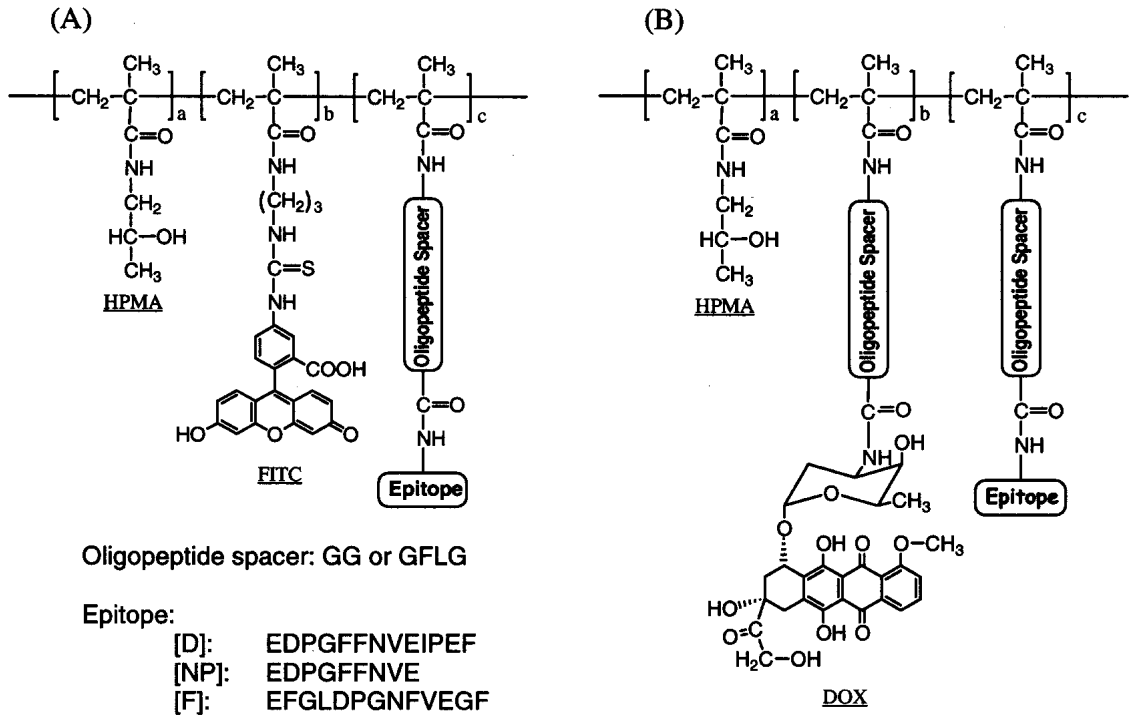


Oligopeptide spacer: GG or GFLG

Epitope:

[D]: EDPGFFNVEIPEF
[NP]: EDPGFFNVE
[F]: EFGLDPGNFVEGF

| Conjugate | Structure [a] | HPMA | FITC | DOX Content | | Epitope Content | |
|---|---|---|---|---|---|---|---|
| | | mol% | mol% | mmol/g | mol% | mmol/g | mol% |
| C1-1 | P–FITC–GG–[D]-1 | 91.3 | 2.1 | — | — | 0.222 | 5.2 |
| C1-2 | P–FITC–GG–[D]-2 | 91.3 | 2.1 | — | — | 0.180 | 3.9 |
| C1-3 | P–FITC–GG–[D]-3 | 91.3 | 2.1 | — | — | 0.111 | 2.1 |
| C1-4 | P–FITC–GG–[D]-4 | 91.3 | 2.1 | — | — | 0.044 | 0.7 |
| C2 | P–FITC–GG–[NP] | 91.3 | 2.1 | — | — | 0.277 | 6.1 |
| C3 | P–FITC–GG–[F] | 91.3 | 2.1 | — | — | 0.217 | 4.9 |
| C4-1 | P–FITC–GFLG–[D]-1 | 90.6 | 2.4 | — | — | 0.214 | 5.6 |
| C4-2 | P–FITC–GFLG–[D]-2 | 90.6 | 2.4 | — | — | 0.143 | 3.2 |
| C4-3 | P–FITC–GFLG–[D]-3 | 90.6 | 2.4 | — | — | 0.039 | 0.7 |
| C5 | P–FITC–GFLG–[NP] | 90.6 | 2.4 | — | — | 0.237 | 5.5 |
| C6 | P–FITC–GFLG–[F] | 90.6 | 2.4 | — | — | 0.232 | 6.1 |
| C7 | P–GG–[D] | 90.6 | — | — | — | 0.301 | 8.3 |
| C8-1 | P–GFLG–DOX–[D]-1 | 92.2 | — | 0.076 | 1.8 | 0.170 | 4.2 |
| C8-2 | P–GFLG–DOX–[D]-2 | 92.2 | — | 0.097 | 2.0 | 0.092 | 1.9 |
| C9 | P–GFLG–DOX–[NP] | 92.2 | — | 0.081 | 1.8 | 0.21 | 4.9 |
| C10 | P–GFLG–DOX–[F] | 92.2 | — | 0.085 | 2.1 | 0.19 | 4.6 |
| C11 | P–GFLG–DOX | 92.2 | — | 0.086 | 1.5 | — | — |

[a] Epitopes are bracketed in order to differentiate from one-letter abbreviations of amino acids.

**Fig. 1.** Structure and composition of HPMA copolymer conjugates. (A) Conjugates (C1 to C6) containing a fluorescent marker (FITC) and different epitopes. Conjugate C7 contains epitope D only. (B) Conjugates (C8 to C10) containing DOX and different epitopes. Conjugate C11 contains DOX only.

(referred to as conjugate C1-1). The exact epitope content was determined by amino acid analysis.

A conjugate with high epitope D content, but without FITC (C7), was synthesized similarly using polymer precursor 3 (PP3).

*Synthesis of Polymer Conjugates Containing DOX and EP*

PP4 was used to synthesize HPMA copolymer–DOX–EP conjugates (Fig. 1B) following a procedure modified from a previously described protocol (17).

PP4, epitope peptides (0.67 equiv of ONp group in PP4), and DOX·HCl (0.33 equiv of ONp group in PP4) were suspended in DMF. DIPEA diluted in DMF was added slowly while stirring. The reaction mixtures were stirred at room temperature in the dark overnight. After residual ONp groups were deactivated, the reaction mixtures were diluted with MeOH. The crude conjugates (C8-1, C9, and C10) were purified by size exclusion chromatography using Sephadex LH-20 resin in MeOH–1% AcOH (at least twice) followed by dialysis and lyophilization. The epitope content of the conjugates was determined by amino acid analysis, and the content of bound DOX by UV/vis spectrophotometry ($\lambda_{max} \sim 485$ nm, $\varepsilon = 11{,}000\ M^{-1}cm^{-1}$).

Conjugate C8-2 containing a lower epitope D content was synthesized similarly using 0.25 and 0.33 ONp equivalent of epitope D and DOX·HCl, respectively.

Conjugate C11 containing only DOX was also synthesized as a nontargeted control.

## Cell-Binding Assay

### *Cell Lines*

Raji B cells ($CD21^+$) were cultured in RPMI 1640 medium supplemented with 10% FBS. HSB-2 T cells ($CD21^-$) were cultured in Iscove's modified Dulbecco's medium (IMDM) supplemented with 10% FBS. Cells were grown at 37°C in a humidified atmosphere with 5% (v/v) $CO_2$ in air.

A previously described protocol (17) was modified and used in cell-binding experiments (see below).

### *Binding Kinetics*

Raji cells were harvested and washed once with incubation buffer, DPBS containing 0.5% BSA and 30 mM $NaN_3$. The cells were resuspended in the incubation buffer, placed in Eppendorf vials, and kept at 4°C for 30 min. Conjugate C1-1 was added at a final concentration of $5 \times 10^{-5}$ M [D] and incubated with the cells at 4°C in the dark on a rotating sample holder. At various time intervals, triplicate samples of cell suspensions were taken. The cells were pelleted, and supernatants carefully removed. After the cells were washed twice with DPBS, the pellets were dissolved in 1 M NaOH at 4°C overnight. The amount of conjugate bound to the cell surface was determined by fluorescence spectrophotometry using known concentrations of C1-1 in 1 M NaOH as standards. Total cell protein was measured by BCA protein assay. The amount of bound conjugate was normalized to the epitope concentration per microgram of cell protein.

### *Binding Equilibrium*

Binding experiments were performed with Raji and HSB-2 cells using conjugates containing FITC and EP.

Raji and HSB-2 cells were resuspended in the incubation buffer ($1 \times 10^6$ cells in 0.2 ml), placed in Eppendorf vials, and kept at 4°C for 30 min. Conjugates in 0.2 ml of incubation buffer were added at various concentrations (triplicate samples for each concentration) and incubated at 4°C for 4 h in the dark on a rotating sample holder. The amounts of bound conjugates were determined as described above. The following equation (Eq. 1) was used to analyze the experimental data:

$$c_{bound} = \frac{K_a \cdot R_T \cdot c_{free}}{1 + K_a \cdot c_{free}} + \alpha \cdot c_{free} \quad (1)$$

where $c_{bound}$ (M epitope/μg protein) and $c_{free}$ (M epitope/μg protein) are concentrations of bound and free conjugates in epitope equivalents. The total concentration of the conjugate was used for $c_{free}$ because the amount of bound conjugate is negligible compared to the total concentration. $K_a$ is the association constant ($M^{-1}$), $R_T$ is the total amount of receptor protein (M/μg protein), and α is a parameter to account for nonspecific interaction of the conjugates with the cell surface.

Nonspecific binding of the conjugates to Raji cells was determined by preincubating the cells with conjugate C7 (1 mM [D]) followed by incubation with different concentrations of conjugates. Linear regression was used to estimate the nonspecific binding parameter α.

## Cytotoxicity Assay

The cytotoxicities of the conjugates containing DOX and EP to Raji and HSB-2 cells were measured by the MTT assay (23). Cells ($10^4$ in 100 μl medium) were seeded into 96-well plates and incubated at cell culture conditions for either 24 h (Raji cells) or 48 h (HSB-2 cells). Conjugates in fresh medium (50 μl) at various concentrations (DOX equiv) were added and incubated with the cells for 72 h and 96 h for Raji and HSB-2 cells, respectively. MTT solution (35 μl of 5 mg/ml in DPBS) was added to each well and incubated under cell culture conditions for 3 h. Extraction/lysing buffer [20% (w/v) SDS in 1:1 (v/v) DMF/water] was then added and incubated at 37°C overnight to dissolve the resulting formazan crystals. The absorbance was measured at 570 nm on a microplate reader (Bio-Rad model 3550, Hercules, CA). For each drug concentration, duplicate drug samples without cells were included as controls, and the background absorbance was subtracted. Cell viabilities relative to untreated control cells were calculated, and the data were used to estimate $IC_{50}$ dose.

## Release of DOX from HPMA Copolymer–DOX Conjugates

Stock solutions of cathepsin B (0.26 mg/ml solid or about 3 μM protein) and GSH (250 mM) were prepared in 0.1 M phosphate buffer (pH 5.5) containing 1 mM EDTA (referred to as PE buffer). The two solutions were mixed at a ratio of 98:2 (v/v) cathepsin B:GSH and incubated at 37°C for 5 min to obtain an enzyme incubation mixture. Conjugates were dissolved in the incubation mixture (at about 300 μM DOX equiv), and the solutions were incubated at 37°C with gentle shaking. At chosen time intervals, duplicate samples (100 μl) were withdrawn, and the released free DOX was extracted with a mixture of 1.0 ml carbonate buffer (0.2 M $Na_2CO_3$/$NaHCO_3$, pH 9.8) and 1.5 ml chloroform. The organic layer was carefully collected and dried with a small amount of drying agent. The concentration of DOX was measured by UV/vis spectrophotometry and the percentage of release was calculated. The activity of the enzyme during the whole experiment was verified with a synthetic substrate Bz-Phe-Val-Arg-NAp.

## RESULTS

### Kinetics of Cell Binding

Conjugate C1-1 (P–FITC–GG–[D]-1) was used as an example to study the cell-binding kinetics of the conjugates to Raji and HSB-2 cells. The incubation conditions (buffer and low temperature) were chosen to suppress internalization of the conjugate. The results indicated that equilibrium was reached in approximately 2 h for both cell lines (Fig. 2).

### Equilibrium Binding of Conjugates to Raji B Cells

Equilibrium binding of all conjugates (Fig. 1) to Raji cells was measured. Experimental data were fitted to Eq. (1) to estimate affinity constants (Table II). Nonspecific binding was determined by saturating cell surface receptors with conjugate C7 (P–GG–[D]) before incubating the cells with various concentrations of conjugates. The amount of nonspecifically bound conjugate was a linear function of conjugate concentration for those with a dipeptide ("GG") spacer. However, saturation seemed to occur for conjugates with a tetrapeptide ("GFLG") spacer despite the presence of blocking conjugate C7. In the first case, the nonspecific adsorption data were approximated with linear regression and parameter $\alpha$ was determined as the slope (data not shown). Specific binding data were then fitted to Eq. (1) with the $\alpha$ value fixed. In the second case, all parameters were determined simultaneously by fitting the data to Eq. (1).

#### *Influence of Epitope Structure on Cell Binding*

Three different epitopes were evaluated: epitopes D, NP, and F. The results for three conjugates with the dipeptide spacer and high epitope content are shown in Fig. 3A. Apparently, these conjugates bound specifically to Raji cells. The conjugate with high epitope D content showed the highest binding affinity to Raji cells (Table II).

Among the conjugates with the tetrapeptide spacer, the one with the highest epitope D content maintained the highest apparent binding affinity to Raji cells. However, the differences in binding affinities for conjugates with different epitopes were diminished compared to the conjugates with the dipeptide spacer (Table II).

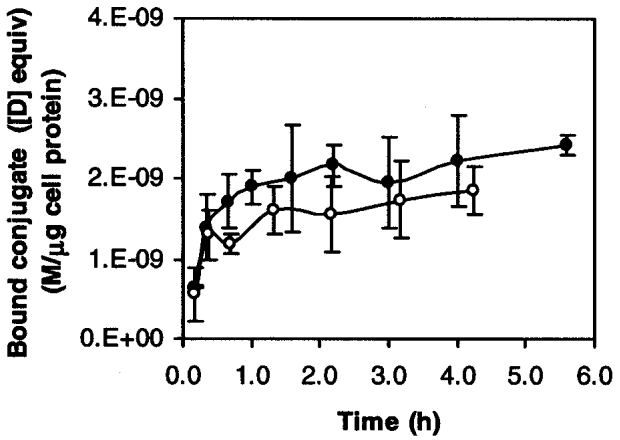


**Fig. 2.** Binding kinetics of conjugate C1-1 to Raji *(filled circle)* and HSB-2 *(open circle)* cells. Data are depicted by mean ± standard deviation from triplicate measurements.

**Table II.** Binding Constants ($K_a$, $10^5$ $M^{-1}$)[a,b] of the Conjugates to Raji and HSB-2 Cells

| Conjugate | Spacer | Epitope | Cell lines | |
|---|---|---|---|---|
| | | | Raji | HSB-2 |
| C1-1 | GG | [D] | 1.64 ± 0.21 | 0.41 ± 0.14 |
| C1-2 | GG | [D] | 0.74 ± 0.09 | 0.24 ± 0.10 |
| C1-3 | GG | [D] | 0.24 ± 0.05 | N/D[c] |
| C1-4 | GG | [D] | 0.21 ± 0.05 | N/D[c] |
| C2 | GG | [NP] | 0.22 ± 0.06 | N/A[d] |
| C3 | GG | [F] | 0.46 ± 0.08 | 0.19 ± 0.06 |
| C4-1 | GFLG | [D] | 1.67 ± 0.34 | 0.44 ± 0.17 |
| C4-2 | GFLG | [D] | 1.02 ± 0.37 | N/D[c] |
| C4-3 | GFLG | [D] | 0.73 ± 0.16 | N/D[c] |
| C5 | GFLG | [NP] | 0.79 ± 0.20 | 0.20 ± 0.10 |
| C6 | GFLG | [F] | 1.20 ± 0.17 | 0.58 ± 0.14 |

[a] The data indicate mean ± error from curve fitting.
[b] Statistics: $p < 0.05$: Raji cell affinity vs. HSB-2 cell affinity for all conjugates studied; $p < 0.05$: C1-1 vs. C1-2, C1-3, C1-4, C2, and C3; C1-2 vs. C1-3, C1-4, and C2; C3 vs. C2 [Raji cell affinity: influence of epitope structure and epitope content ("GG" spacer)]; $p < 0.05$: C4-1 vs. C4-3, C5 [Raji cell affinity: influence of epitope structure and epitope content ("GFLG" spacer)]; $p < 0.05$: C4-3 vs. C1-4; C5 vs. C2; C6 vs. C3 (Raji cell affinity: influence of conjugation spacer).
[c] N/D: Not determined.
[d] N/A: Not available because of absence of specific binding pattern.

#### *Influence of Epitope Content on Cell Binding*

Four conjugates with the dipeptide spacer and different epitope D contents were studied (Fig. 3B and Table II). Increasing the epitope content resulted in a higher cell-binding affinity. The apparent binding constant of conjugate C1-1 (containing 5.2 mol% or about five epitope molecules per polymer chain) was about sevenfold higher than that of conjugate C1-3 (containing 2.1 mol% or about two epitope molecules per polymer chain). This may be indicative of a weak multivalency effect.

For conjugates with the tetrapeptide spacer, three epitope compositions were evaluated (C4-1 to C4-3). Similar to the observation for the conjugates with different epitopes bound via the tetrapeptide spacer, the apparent cell-binding affinities became closer to each other when compared to conjugates with the dipeptide spacer (Table II).

#### *Influence of Spacer Structure on Cell Binding*

Two oligopeptide spacers, a dipeptide ("GG") and tetrapeptide ("GFLG"), were investigated. The affinity constant data (Table II) indicated that use of a longer spacer resulted in an apparent increase in Raji cell-binding affinity (C4-3 vs. C1-4, C5 vs. C2, C6 vs. C3) for conjugates with low epitope D content (C1-4) and high epitope NP (C2) and F contents (C3). In other words, Raji cell binding was improved by replacing the "GG" spacer with the "GFLG" spacer only when the initial cell-binding affinities were relatively low. The use of tetrapeptide spacer had little effect for conjugates with higher binding affinities (C4-1 vs. C1-1 and C4-2 vs. C1-2).

### Equilibrium Binding of Conjugates to HSB-2 T Cells

Equilibrium binding of selected conjugates to HSB-2 cells was studied using methods similar to those used in Raji

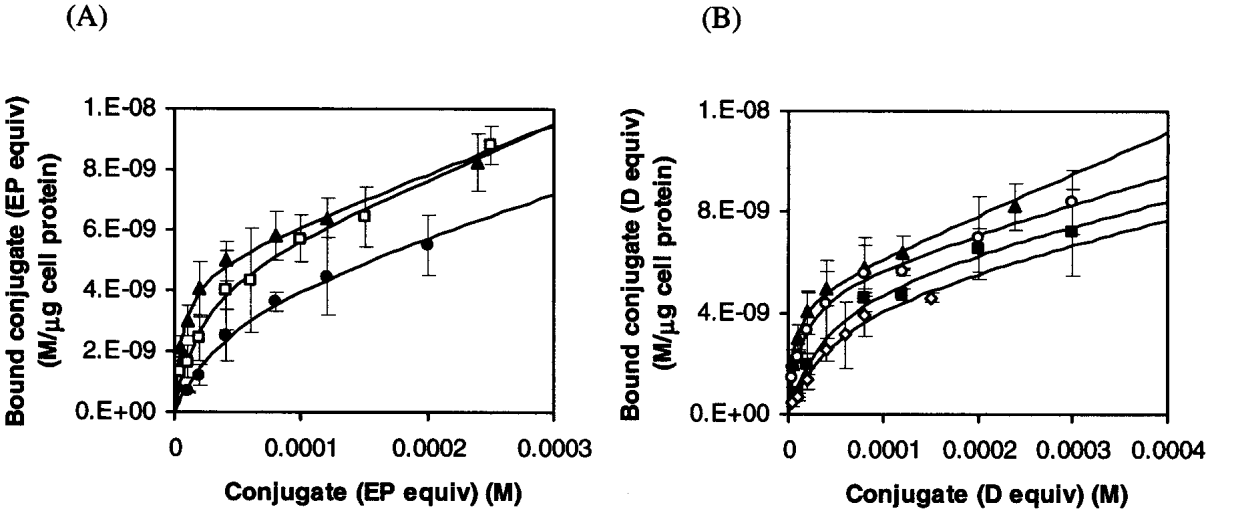


**Fig. 3.** Influence of epitope structure and content on Raji cell-binding affinity. Data are depicted by mean ± standard deviation from triplicate measurements. (A) Equilibrium binding curves of conjugates containing different epitopes bound to the polymer backbone via "GG" spacer: C1-1 (▲), C2 (●), and C3 (□). (B) Equilibrium binding curves of conjugates containing different amounts of epitope D bound to the polymer backbone via "GG" spacer: C1-1 (▲), C1-2 (○), C1-3 (■), C1-4 (◇).

cell-binding experiments (Table II). Generally, these conjugates bound to HSB-2 cell at lower affinities relative to Raji cells. The differences in epitope structure and epitope content did not significantly affect the binding constants ($p > 0.05$).

### Cytotoxicity of Conjugates to Raji and HSB-2 Cells

Dose-dependent growth inhibition of Raji and HSB-2 cells by the conjugates containing DOX and different epitopes (Fig. 1) was measured. Because of the longer lag phase of HSB-2 cell growth in microplate wells, the experiment protocol was slightly modified for HSB-2 cells (48 h preincubation and 96 h drug incubation). Polymer-bound DOX had higher apparent $IC_{50}$ values relative to the free drug. For both cell lines, incorporation of a small amount of epitope D in the conjugate (C8-2) resulted in little improvement in cytotoxicity compared to the conjugate without the epitope (C11, nontargeted conjugate). In contrast, the conjugate with a higher epitope D content (C8-1) demonstrated a significantly higher toxicity to both cells relative to the nontargeted conjugate (Fig. 4). HSB-2 T cells were more sensitive to DOX than Raji B cells, as indicated by lower $IC_{50}$ values. However, the enhancement in cytotoxicity of targeted conjugate (C8-1) over nontargeted conjugate (C11) was more pronounced for Raji cells (44-fold) than for HSB-2 cells (12-fold). D and NP Conjugates (C8-1 and C9) showed similar $IC_{50}$ values for both cell lines. On the other hand, D conjugate (C8-1) was slightly more toxic to Raji cells than F conjugate (C10), whereas both D and NP conjugates (C8-1 and C9) were slightly more toxic to HSB-2 cells than F conjugate (Table III).

### *In Vitro* DOX Release

Cathepsin B is an important cysteine protease responsible for hydrolysis of proteins and the "GFLG" spacer used in HPMA copolymer–drug conjugates in lysosomal compartments of the cells (24). It was used to evaluate the rates of *in vitro* cleavage of the tetrapeptide spacer and release of DOX from different conjugates. All conjugates showed a similar DOX release pattern. Nearly 40% of DOX was released from these conjugates after 45 h of incubation at 37°C (Fig. 5).

## DISCUSSION

### Epitope-Mediated Cell Binding

The results from the cell-binding experiments showed that epitope-containing HPMA copolymer conjugates bound specifically to $CD21^+$ Raji cells with different affinities depending on epitope structure. The ability of conjugate C7, containing only epitope D, to block specific bindings of conjugates with "GG" spacer and different epitopes (C1-1 to C3) clearly indicated that the binding was mediated by the epitopes that were covalently bound to the polymer backbone and that the CD21 receptor was probably involved. These conjugates also bound to HSB-2 T cells that did not express the CD21 receptor, but at lower affinities than to Raji cells. This observation is consistent with a previous study on the binding of microspheres containing covalently bound NP epitope to Raji and HSB-2 cells (16). The results showed that 47–76% of Raji cells bound to the microspheres, whereas only 11% of HSB-2 cells were bound. The binding of polymer conjugates to HSB-2 cells was likely a combination of nonspecific interactions and/or perhaps specific binding involving receptors other than CD21. HSB-2 cells have been shown to express an EBV receptor with phenotypic characteristics distinct from CD21 (25). This receptor interacts with EBV via the N-terminal portion of the viral envelope glycoprotein gp350/220 (26). It is thus possible that the epitope-containing conjugates interacted with the HSB-2 cells via the EBV receptor.

Among the conjugates containing different epitopes, the ones with epitope D showed the highest apparent affinity to Raji cells (Table II). This is consistent with a previous result from studies on the recognition of epitopes incorporated in coiled-coil stem loop peptides by purified soluble CD21 receptor and CD21-bearing Raji cells (18). This suggests that

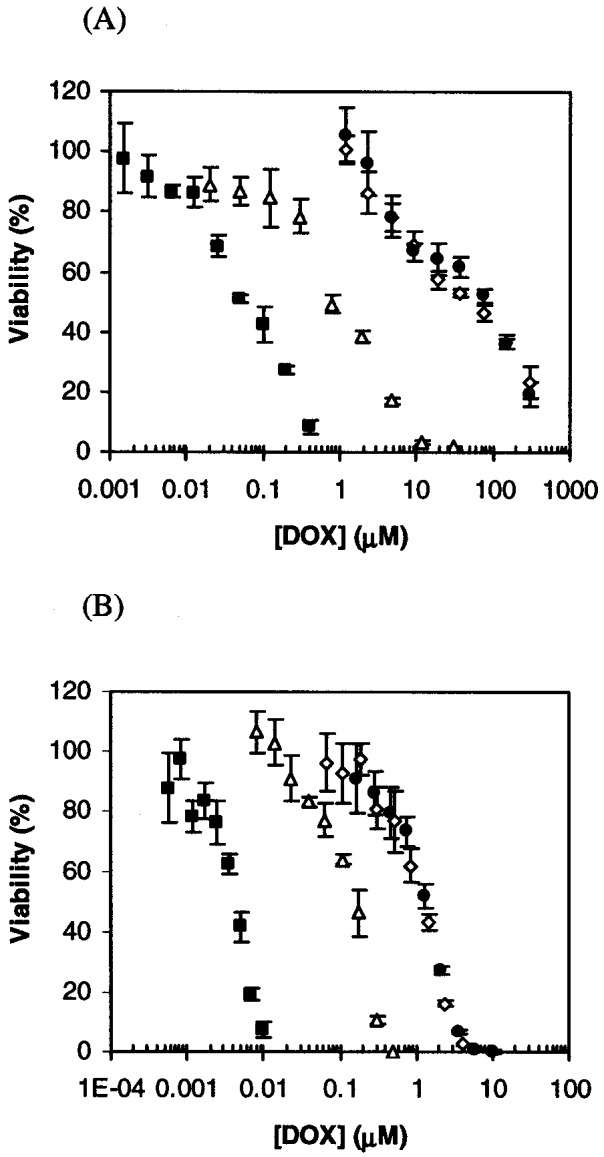


**Fig. 4.** Inhibition of cell growth by free DOX (■) and polymer-bound DOX: conjugates C8-1 (△), C8-2 (◇), and C11 (●). Data points are depicted by mean ± standard deviation from quadruplicate measurements. (A) $CD21^+$ Raji cells. (B) $CD21^-$ HSB-2 cells.

biorecognition studies of epitopes presented on coiled-coil stem loop peptides might be useful in predicting the binding of epitope-containing polymer conjugates to receptor-bearing cells.

Studies on the interaction of CD21 receptor with its natural ligand, complement component C3dg, indicated that high-avidity binding to CD21 required multimerization of ligand (27–29) and implied clustering of the receptor on the cell surface (30). Multivalent interactions of cell surface CD21 receptor with C3dg ligand suggest that this receptor can interact in a similar manner with HPMA copolymer conjugates containing multiple epitope molecules. In addition to possible multivalent interactions, the larger affinity constants associated with higher epitope content observed in this study might also reflect a higher local concentration of the epitope and, hence, an increased binding avidity.

**Table III.** $IC_{50}$ Doses (μM)[a] of Free and Polymer-Bound DOX for Raji and HSB-2 Cells

| Drug | Structure | Cell lines | |
|---|---|---|---|
| | | Raji | HSB-2 |
| DOX | Free DOX | 0.0644 ± 0.0087 | 0.00383 ± 0.0002 |
| C8-1 | P–GFLG–DOX–[D]–1 | 1.18 ± 0.34[b,c] | 0.115 ± 0.007[d,e] |
| C8-2 | P–GFLG–DOX–[D]–2 | 42.3 ± 3.01[b] | 1.16 ± 0.200 |
| C9 | P–GFLG–DOX–[NP] | 2.28 ± 0.39[b] | 0.128 ± 0.003[d,e] |
| C10 | P–GFLG–DOX–[F] | 4.37 ± 0.71[b] | 0.270 ± 0.040[d] |
| C11 | P–GFLG–DOX | 52.3 ± 0.42 | 1.34 ± 0.023 |

[a] Data indicate mean ± standard deviation from two independent experiments, each with quadruplicate samples.
[b] $p < 0.05$ compared to conjugate C11 for Raji cells.
[c] $p < 0.05$ compared to conjugate C10 for Raji cells.
[d] $p < 0.05$ compared to conjugate C11 for HSB-2 cells.
[e] $p < 0.05$ compared to conjugate C10 for HSB-2 cells.

### Epitope-Mediated Cytotoxicity

In all HPMA copolymer–DOX conjugates, DOX was coupled to the polymer backbone via the "GFLG" spacer, which was cleavable by lysosomal enzymes, resulting in release of free DOX (2,25). Polymer-bound DOX showed lower apparent cytotoxicities relative to free DOX because of lower efficiency of cell entry through pinocytosis (2). The dramatic improvement in cytotoxicities of the targeted conjugates vs. the nontargeted conjugate was consistent with previously proposed mechanisms of cell entry (2), i.e., receptor-mediated pinocytosis for the targeted conjugates or slower fluid-phase and/or adsorptive pinocytosis for the nontargeted conjugate. Although HSB-2 cells were more sensitive to both free and polymer-bound DOX than Raji cells, the enhancement in toxicity by incorporating targeting moieties was more pronounced for Raji cells (Table III). This observation seemed to agree with equilibrium binding experiments showing that epitope-containing polymer conjugates possessed

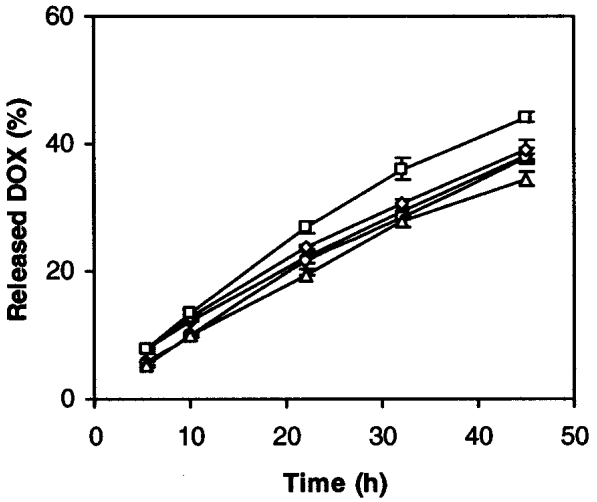


**Fig. 5.** *In vitro* release of DOX from HPMA copolymer–DOX conjugates catalyzed by cathepsin B at 37°C. Initial concentrations of DOX in the conjugates were 314 (C8-1, ♦), 311 (C8-2, ○), 302 (C9, ◇), 300 (C10, □), and 300 μM (C11, △). Data points are depicted by mean ± error from duplicate measurements. Some error bars are too small to be seen.

higher apparent affinities for Raji cells than for HSB-2 cells (Table II).

Several factors may influence the intracellular concentration of functional DOX and hence cytotoxicity of the conjugates: the rate of conjugate internalization, rate of DOX release from the conjugate, and transport of released free DOX from the lysosomes into the cytoplasm and, finally, into the nucleus. Among these factors, the first two may contribute to different cytotoxicities of the conjugates. Because all conjugates possessed similar DOX release rates (Fig. 5), the differences in apparent cytotoxicities of these conjugates may be attributed to different rates of conjugate internalization. Thus, the higher cytotoxicities of the targeted conjugates relative to the nontargeted conjugate and the conjugate containing a low amount of epitope most likely reflected an enhanced internalization of the conjugates through receptor-mediated endocytosis after effective binding of the conjugates to the cell surface. The slightly lower cytotoxicity of F conjugate relative to D and NP conjugates probably resulted from different conjugate internalization rates due to subtle differences in conjugate structure.

## ACKNOWLEDGMENTS

This work was supported in part by NIH Grant CA88047 from the National Cancer Institute. We thank Dr. M. Pechar (Institute of Macromolecular Chemistry, Czech Republic) for advice on solid-phase peptide synthesis.

## REFERENCES

1. The Leukemia & Lymphoma Society. http://www.leukemia-lymphoma.org.
2. D. Putnam and J. Kopeček. Polymer conjugates with anticancer activity. *Adv. Polym. Sci.* **122**:55–123 (1995).
3. J. Kopeček, P. Kopečková, T. Minko, and Z. Lu. HPMA copolymer-anticancer drug conjugates: design, activity, and mechanism of action. *Eur. J. Pharm. Biopharm.* **50**:61–81 (2000).
4. H. Maeda, L. W. Seymour, and Y. Miyamoto. Conjugates of anticancer agents and polymers: advantages of macromolecular therapeutics *in vivo*. *Bioconjug. Chem.* **3**:351–362 (1992).
5. T. Minko, P. Kopečková, V. Pozharov, and J. Kopeček. HPMA copolymer bound adriamycin overcomes MDR1 gene encoded resistance in a human ovarian carcinoma cell line. *J. Control. Release* **54**:223–233 (1998).
6. T. Minko, P. Kopečková, and J. Kopeček. Comparison of the anticancer effect of free and HPMA copolymer-bound adriamycin in human ovarian carcinoma cells. *Pharm. Res.* **16**:986–996 (1999).
7. T. Minko, P. Kopečková, and J. Kopeček. Efficacy of the chemotherapeutic action of HPMA copolymer-bound doxorubicin in a solid tumor model of ovarian carcinoma. *Int. J. Cancer* **86**:108–117 (2000).
8. R. C. Rath, P. Kopečková, and J. Kopeček. Biorecognition of sugar containing N-(2-hydroxypropyl)methacrylamide copolymers by immobilized lectin. *Macromol. Chem. Phys.* **198**:1165–1180 (1997).
9. B. Říhová, P. Kopečková, J. Strohalm, P. Rossmann, V. Větvička, and J. Kopeček. Antibody-directed affinity therapy applied to the immune system: *in vivo* effectiveness and limited toxicity of daunomycin conjugated to HPMA copolymers and targeting antibody. *Clin. Immunol. Immunopathol.* **46**:100–114 (1988).
10. Z. R. Lu, P. Kopečková, and J. Kopeček. Polymerizable Fab′ antibody fragments for targeting of anticancer drugs. *Nat. Biotechnol.* **17**:1101–1104 (1999).
11. T. F. Tedder, L. T. Clement, and M. D. Cooper. Expression of C3d receptors during human B cell differentiation: immunofluorescence analysis with the HB-5 monoclonal antibody. *J. Immunol.* **133**:678–683 (1984).
12. E. Fischer, C. Delibrias, and M. D. Kazatchkine. Expression of CR2 (the C3dg/EBV receptor, CD21) on normal human peripheral blood T lymphocytes. *J. Immunol.* **146**:865–869 (1991).
13. R. Rask, J. M. Rasmussen, H. V. Hansen, P. Bysted, and S.-E. Svehag. Complement C3d,g/Epstein–Barr virus receptor density on human B-lymphocytes estimated by immunoenzymatic assay and immunocytochemistry. *J. Clin. Lab. Immunol.* **25**:153–156 (1988).
14. G. Sauvageau, R. Stocco, S. Kasparian, and J. Menezes. Epstein–Barr virus (EBV) receptor expression on human $CD8^+$ (cytotoxic/suppressor) T lymphocytes. *J. Gen. Virol.* **71**:379–386 (1990).
15. G. R. Nemerow, C. Mold, V. K. Schwend, V. Tollefson, and N. R. Cooper. Identification of gp350 as the viral glycoprotein mediating attachment of Epstein–Barr virus (EBV) to the EBV/C3d receptor of B cells: sequence homology of gp350 and C3 complement fragment C3d. *J. Virol.* **61**:1416–1420 (1987).
16. G. R. Nemerow, R. A. Houghten, M. D. Moore, and N. R. Cooper. Identification of an epitope in the major envelope protein of Epstein–Barr virus that mediates viral binding to the B lymphocyte EBV receptor (CR2). *Cell* **56**:369–377 (1989).
17. V. Omelyanenko, P. Kopečková, R. K. Prakash, C. D. Ebert, and J. Kopeček. Biorecognition of HPMA copolymer–adriamycin conjugates by lymphocytes mediated by synthetic receptor binding epitopes. *Pharm. Res.* **16**:1010–1019 (1999).
18. A. Tang. and J. Kopeček. Presentation of epitopes on genetically engineered peptides and selection of lymphoma-targeting moieties based on epitope biorecognition. *Biomacromolecules* **3**:421–431 (2002).
19. J. Kopeček and H. Bažilová. Poly[N-(2-hydroxypropyl)methacrylamide]-I. Radical polymerization and copolymerization. *Eur. Polym. J.* **9**:7–14 (1973).
20. P. Rejmanová, J. Labský, and J. Kopeček. Aminolyses of monomeric and polymeric *p*-nitrophenol esters of methacryloylated amino acids. *Makromol. Chem.* **178**:2159–2168 (1977).
21. K. Ulbrich, V. Šubr, J. Strohalm, D. Plocová, M. Jelínková, and B. Říhová. Polymeric drugs based on conjugates of synthetic and natural macromolecules. I. Synthesis and physico-chemical characterisation. *J. Control. Release* **64**:63–79 (2000).
22. V. Omelyanenko, P. Kopečková, C. Gentry, and J. Kopeček. Targetable HPMA copolymer–adriamycin conjugates. Recognition, internalization, and subcellular fate. *J. Control. Release* **53**:25–37 (1998).
23. M. B. Hansen, S. E. Nielsen, and K. Berg. Re-examination and further development of a precise and rapid dye method for measuring cell growth/cell kill. *J. Immunol. Methods* **119**:203–210 (1989).
24. P. Rejmanová, J. Kopeček, J. Pohl, M. Baudyš, and V. Kostka. Polymers containing enzymatically degradble bonds 8. Degradation of oligopeptide sequences in N-(2-hydroxypropyl)methacrylamide copolymers by bovine spleen cathepsin B. *Makromol. Chem.* **184**:2009–2020 (1983).
25. J. A. Hedrick, D. Watry, C. Speiser, P. O'Donnell, J. D. Lambris, and C. D. Tsoukas. Interaction between Epstein–Barr virus and a T cell line (HSB-2) via a receptor phenotypically distinct from complement receptor type 2. *Eur. J. Immunol.* **22**:1123–1131 (1992).
26. J. A. Hedrick, Z. Lao, S. G. Lipps, Y. Wang, S. C. Todd, J. D. Lambris, and C. D. Tsoukas. Characterization of a 70-kDa, EBV gp350/220-binding protein on HSB-2 T cells. *J. Immunol.* **153**:4418–4426 (1994).
27. M. D. Moore, R. G. DiScipio, N. R. Cooper, and G. R. Nemerow. Hydrodynamic, electron microscopic, and ligand-binding analysis of the Epstein–Barr virus/C3dg receptor (CR2). *J. Biol. Chem.* **264**:20576–20582 (1989).
28. C. A. Lowell, L. B. Klickstein, R. H. Carter, J. A. Mitchell, D. T. Fearon, and J. M. Ahearn. Mapping of the Epstein–Barr virus and C3dg binding sites to a common domain on complement receptor type 2. *J. Exp. Med.* **170**:1931–1946 (1989).
29. S. E. Henson, D. Smith, S. A. Boackle, V. M. Holers, and D. R. Karp. Generation of recombinant human C3dg tetramers for the analysis of CD21 binding and function. *J. Immunol. Methods* **258**:97–109 (2001).
30. M. W. Hess, M. G. Schwendinger, E. L. Eskelinen, K. Pfaller, M. Pavelka, M. P. Dierich, and W. M. Prodinger. Tracing uptake of C3dg-conjugated antigen into B cells via complement receptor type 2 (CR2, CD21). *Blood* **95**:2617–2623 (2000).